ORIGINAL ARTICLE

Diagnostic Value of Dynamic Contrast-Enhanced (DCE), Dynamic Susceptibility Contrast (DSC) and Arterial Spin Labeling (ASL) Perfusion MRI for Differentiation of High-Grade and Low-Grade Gliomas

Oranan Tritanon, MD[1], Wisinee Boonsang, MD[1], Thanissara Chansakul, MD[1], Panitha Jindahra, MD, PhD[2], Theeraphol Panyaping, MD[1]

[1] Division of Diagnostic Neuroradiology, Department of Diagnostic and Therapeutic Radiology, Faculty of Medicine, Ramathibodi Hospital, Mahidol University, Bangkok, Thailand; [2] Department of Medicine, Faculty of Medicine, Ramathibodi Hospital, Mahidol University, Bangkok, Thailand

Objective: To evaluate dynamic contrast-enhanced (DCE), dynamic susceptibility contrast (DSC), and arterial spin labeling (ASL)-derived perfusion magnetic resonance imaging (MRI) parameters as a non-invasive technique for differentiating between high-grade gliomas (HGGs) and low-grade gliomas (LGGs), and to determine the diagnostic value of each parameter.

Materials and Methods: Twenty-four patients with histopathologically confirmed HGGs or LGGs underwent DCE-, DSC-, and ASL-magnetic resonance perfusion (MRP). Retrospective qualitative and quantitative assessment of MRP-derived parameters, including DCE-K^{trans}, DCE-V_e, DCE-V_p, DSC-rCBV, DSC-rCBF, and ASL-rCBF were performed, and the diagnostic value of each parameter was determined using ROC analysis.

Results: Of the 24 patients enrolled in the present study, which included 10 LGGs and 14 HGGs, DCE-derived V_p showed the best diagnostic performance for differentiating between HGGs and LGGs (AUC 0.833, cutoff >0.0002 mL/100 g, p=0.018, 100% sensitivity, 28.6% specificity), followed by DCE-derived K^{trans} (AUC 0.75, cutoff >0.024 min^{-1}, p=0.011, 58.3% sensitivity, 100% specificity) and DSC-derived normalized rCBV (AUC 0.75, p=0.021, cutoff >1.15, 100% sensitivity, 37.5% specificity). The ASL-derived normalized rCBF showed no statistically significant difference between HGGs and LGGs (AUC 0.457, p=0.757).

Conclusion: DCE-derived V_p, DCE-derived K^{trans}, and DSC-derived rCBV are helpful perfusion MRI parameters for differentiating HGGs and LGGs, with DCE-derived V_p showing the best diagnostic performance in the present study.

Keywords: DCE; DSL; ASL; Perfusion MR; Glioma

Received 13 September 2022 | Revised 27 February 2023 | Accepted 27 February 2023

J Med Assoc Thai 2023;106(5):476-86

Website: http://www.jmatonline.com

Gliomas account for approximately 25% of all central nervous system tumors and 80% of all malignant brain tumors[1]. The 2021 World Health Organization (WHO) classification divides gliomas based on genetic appearance. IDH-mutant astrocytomas are classified into grades 2 to 4[2]. Grades 2 are considered low-grade gliomas (LGGs), and grades 3 and 4 suggest high-grade gliomas (HGGs).

Management of HGGs usually involves aggressive treatment, including maximal safe resection to improve survival, followed by adjuvant treatment with radiation and chemotherapy. LGGs are usually closely followed without the symptomatic need for surgery because of their typically indolent clinical course[3,4].

The biopsy is the gold standard to determine tumor grade before starting treatment, but there are limitations in clinical practice. For example, it is an invasive procedure that carries risks of morbidity and is sometimes not feasible in eloquent areas or difficult-to-access locations. In addition, the biopsy is also susceptible to inherent sampling error. Hence, non-invasive diagnosis with brain magnetic

Correspondence to:

Panyaping T.

Division of Diagnostic Neuroradiology, Department of Diagnostic and Therapeutic Radiology, Faculty of Medicine, Ramathibodi Hospital, Mahidol University, 270 Rama VI Road, Phayathai, Ratchathewi, Bangkok 10400, Thailand.

Phone: +66-2-2011212, **Fax**: +66-2-2011297

Email: theeraphol1@gmail.com

How to cite this article:

Tritanon O, Boonsang W, Chansakul T, Jindahra P, Panyaping T. Diagnostic Value of Dynamic Contrast-Enhanced (DCE), Dynamic Susceptibility Contrast (DSC) and Arterial Spin Labeling (ASL) Perfusion MRI for Differentiation of High-Grade and Low-Grade Gliomas. J Med Assoc Thai 2023;106:476-86.

DOI: 10.35755/jmedassocthai.2023.05.13845

resonance imaging (MRI) is crucial in guiding therapy in such cases. As conventional MRIs are not always precise in differentiating HGGs from LGGs, pre-treatment imaging with perfusion MRI plays an important role not only in assessing tumor grade but also in suggesting target areas of highest yield for tumor biopsy[4].

Magnetic resonance perfusion (MRP) can be performed with different techniques, including dynamic contrast-enhanced (DCE), dynamic susceptibility contrast (DSC), and arterial spin labeling (ASL) techniques. The most commonly performed MRP technique in clinical practice is DSC-MRP. However, it has been shown that DCE-MRP may provide added benefits of higher spatial resolution, more reliable quantification measurement of microvasculature and permeability indices, and reduced susceptibility artifacts with respect to DSC-MRI[5].

Previous studies on the diagnostic value of DSC-derived and DCE-derived parameters in differentiating HGGs and LGGs showed differing data. Studies revealed that DCE-derived parameters could differentiate between LGGs and HGGs with high accuracy[5-11]. For instance, Arevalo-Perez et al.[12] showed that DCE parameters have high sensitivity and specificity for differentiation of LGGs and HGGs with the fractional blood plasma volume (V_p) mean yielding the highest area under the curve (AUC) of 0.97, 95% sensitivity, and 90.7% specificity and demonstrating good correlation with DCE-derived volume transfer coefficient (K^{trans}) mean, which demonstrated 79.1% sensitivity and 95.0% specificity. The DSC-derived parameters also have been shown to correlate well with glioma grades, although with a lower AUC of 0.78, a sensitivity of 97%, and a specificity of 67%[13]. Most of the previous studies revealed that the DCE-derived parameters, including K^{trans}, V_p, and volume fraction of extravascular extracellular space (V_e) have higher or similar diagnostic performance compared to that of DSC-derived parameters as relative cerebral blood volume (rCBV) and relative cerebral blood flow (rCBF) in differentiating between HGGs and LGGs on preoperative imaging[4,13,14]. However, previous studies showed that both DCE-derived and DSC-derived parameters are reliable techniques, and rCBV was the most sensitive parameter[15].

Previous studies showed that ASL-derived rCBF also correlated well with DSC-derived rCBF and had high diagnostic performance in differentiation between HGGs and LGGs. This technique might be beneficial in patients with contraindications for gadolinium-based contrast agents[16-20].

The purpose of the present study was to evaluate DCE-, DSC-, and ASL-derived MRP parameters for differentiation between HGGs and LGGs and to determine the diagnostic values of each parameter.

Materials and Methods

Patient population

The present study was a retrospective cross-sectional study conducted in the Department of Diagnostic and Therapeutic Radiology of Ramathibodi Hospital and was approved by the Institutional Ethics Committee (COA. MURA2020/1627).

Twenty-four patients with pathologically confirmed glioma were referred for 1.5T or 3T MRI before starting treatment between January 2015 and August 2020. Inclusion criteria included 1) patients had at least two MRP techniques (DCE, DSC, or ASL), and 2) surgical resection or biopsy showing LGG (WHO grade 1 and 2) or HGG (WHO grade 3 and 4), according to the 2016 WHO classification of tumors of the central nervous system[21].

Exclusion criteria include 1) the presence of marked hemorrhage within the tumors causing extensive susceptibility artifact, 2) patients who received any treatment such as chemotherapy or radiation therapy or underwent biopsy/surgery before the MRI, 3) the absence of a histopathologic diagnosis, and 4) inadequate MRP techniques.

The electronic medical records of all patients were also retrospectively reviewed.

MRI protocols and data acquisition

All patients were examined with the same imaging acquisition protocol on 1.5T and 3T scanners (Ingenia, Philips Healthcare, Best, the Netherlands) using a 15-channel receiver head coil. MR sequences were performed according to the standard protocol, including sagittal T1-weighted image (T1W), axial T2-weighted image with fat suppression (T2W/FS), diffusion-weighted image (DWI) with b values of 0 and 1,000 s/mm², axial T1W, and coronal fast field echo (FFE) T2W.

Firstly, ASL-MRP was performed using the 3D pseudo-continuous arterial spin labeling (PCASL) technique before gadolinium-based contrast administration. The imaging parameters were as follows: TR/TE=4,234/11 ms, inversion time (post label delay)=2,000 ms, flip angle 90°, FOV=240×240 mm, matrix=64×60 mm, slice thickness=6.0 mm, number of dynamic scans=8. The total acquisition

time was 4 minutes and 56 seconds.

After that, a cumulative dose of 0.1 mmol/kg of gadobutrol (Gadovist, 1 mmol/mL, Bayer Schering Pharma, Berlin, Germany) was administered, split into two boluses of 0.05 mmol/kg. The first bolus of 0.05 mmol/kg was injected 50 seconds after the start of the DCE sequence by using a power injector at a rate of 5 mL/second and immediately followed by a 30 mL continuous saline flush. The DCE-MRP was performed with an axial FFE T1W sequence using the following parameters: TR/TE=2.8/1.32 ms, flip angle 10°, FOV=200×200 mm, matrix=100×100 mm, slice thickness=2.5 mm, number of dynamic scans=120. The total acquisition time was 5 minutes and 16 seconds. The DCE-MRP was preceded by a variable flip angle axial sequence (5°/10°/15°) for T1 mapping.

Then, the second bolus of 0.05 mmol/kg was injected 40 seconds after the start of the DSC sequence by using the same power injector, rate of injection, and amount of saline flush. Note that the contrast administration during the DCE sequence pre-loaded the tissue for the following DSC sequence. The DSC-MRP was performed with an axial FFE T2*-weighted EPI sequence using the following parameters: TR/TE=1,345/35 ms, flip angle=30°, FOV=240×240 mm, matrix=80×79 mm, slice thickness=5.0 mm, number of dynamic scans=120. The total acquisition time was 2 minutes and 45 seconds.

Post-contrast MR sequences, including contrast-enhanced 3-dimensional fluid-attenuated inversion recovery with fat suppression (CE-3D FLAIR/FS), contrast-enhanced 3-dimensional spoiled gradient-echo high-resolution T1W (CE-3D THRIVE), and contrast-enhanced T1W (CE-T1W) were subsequently obtained as parts of the routine standard protocol.

Post-processing of MRP images and data analysis

DCE-, DSC-, and ASL-MRP data of each patient were processed on a workstation using the IntelliSpace Portal 8.0 software (Philips) with automated generation of perfusion parametric maps, including parametric maps of K^{trans}, V_e, and V_p from DCE-MRP, parametric maps of rCBV and rCBF from DSC-MRP, as well as parametric maps of rCBF from ASL-MRP.

Post-processing perfusion parametric maps and quantitative perfusion data of DCE-derived K^{trans}, V_e, and V_p were verified to match the injection condition during acquisition. In DCE, parametric maps of K^{trans}, V_e, and V_p maps were calculated using the extended two-compartment pharmacokinetic Tofts and Kermode's model[14,22]. Deconvolution with arterial input function (AIF) was performed. The AIF was measured from a region of interest (ROI) placed in the middle cerebral artery of each patient.

Post-processing parametric maps and quantitative perfusion data of DSC-derived rCBV and rCBF were performed without leakage correction. In DSC, parametric maps of rCBV and rCBF were calculated using a tracer kinetic model applied to the first-pass of bolus and generated signal intensity-time curve. The signal intensity-time curve was converted into a relative tracer tissue concentration-time curve and analyzed the hemodynamic parameters[23].

Qualitative imaging analysis

Two neuroradiologists (OT) and (TP) with 12 and 13 years of neuroimaging experience, blinded to clinical information and histopathological diagnosis, independently reviewed both MRI and visual inspection on perfusion parametric maps of all patients on a PACS workstation. Tumor characteristics on MRI were evaluated for tumor margin, T2/FLAIR mismatch[24], cystic/necrotic portion, internal hemorrhage/calcification, intratumoral signal void, restricted diffusion, and enhancement pattern. The tumor margin was grouped as well-defined and infiltrative. The presence or absence of T2/FLAIR mismatch, cystic/necrotic portion, internal hemorrhage/calcification, intratumoral signal void, and restricted diffusion were identified. Enhancement patterns were classified as absence, homogenous enhancement, heterogeneous enhancement, or ring enhancement.

Each perfusion parametric map from each patient was determined as the presence or absence of hyperperfusion area or increased permeability compared to the contralateral normal-appearing cerebral white matter (NAWM). If there was a discordant result among the reviewers, the consensus agreement was discussed in an additional evaluating session.

Quantitative imaging analysis

ROIs were manually drawn by the second-year in-training neuroradiology fellow (WB) blinded to clinical information and histopathological diagnosis. The ROIs were drawn at the highest value of each perfusion parametric map, including parametric maps of K^{trans}, V_e, and V_p from DCE-MRP, parametric maps of rCBV and rCBF from DSC-MRP, and parametric maps of rCBF from ASL-MRP. Three ROIs per selected consecutive slices where the tumor can

be visualized were placed over the solid part of the tumor, avoiding the areas of vessel, calcification, hemorrhage, cyst, and necrosis. CE-3D FLAIR/FS, T2W/FS, and CE-3D THRIVE sequences were used to guide the placement of ROIs to avoid the lesion edge, cyst, necrosis, hemorrhage, and calcification. The area of the ROI was at least 10 mm^2. The perfusion parameters were automatically calculated on IntelliSpace Portal 8.0 software (Philips). The highest perfusion value on each parametric map was selected.

Another ROI was drawn over the contralateral NAWM. The normalized value of tumor-to-contralateral NAWM was determined for parametric maps of rCBV and rCBF on the DSC-MRP and rCBF on the ASL-MRP using the following equation.

$$\text{The normalized perfusion value} = \frac{\text{ROI (tumor)}}{\text{ROI (contralateral NAWM)}}$$

Statistical analysis

The data were statistically analyzed using Stata Statistical Software, version 15.1 (StataCorp LLC, College Station, TX, USA). Clinical characteristics and histopathology of all patients were represented as relative percentages. Independent sample t-test for continuous variables and chi-square test for categorical variables were used to compare demographic data, MRI characteristics and perfusion in parametric maps between patients with LGG and HGG. A p-value less than 0.05 was considered significant.

Receiver operating characteristic (ROC) curve analysis was performed to determine the performance of each perfusion parameter by comparing the AUC. Sensitivity, specificity, positive predictive value (PPV), negative predictive value (NPV), and percentage accuracy of each perfusion parameter for differentiation of LGG and HGG were calculated from parametric maps on both qualitative and quantitative data.

Cohen's Kappa analysis was used to determine interobserver agreement for MR characteristics and perfusion/permeability data on parametric maps. The agreement was interpreted as 0.00 to 0.20 indicates slight agreement, 0.21 to 0.40 indicates fair agreement, 0.41 to 0.60 indicates moderate agreement, 0.61 to 0.80 indicates substantial agreement, and 0.81 to 1.00 indicates almost perfect agreement.

Results

The 24 patients enrolled in the present study had a mean age (±SD) of 52.20±20.09 years, and a range of 17 to 84 years. It included seven males and 17 females. There were 10 LGGs, WHO grade 1 and 2 (41.67%), and 14 HGGs, WHO grade 3 and 4 (58.33%). Demographic data are summarized in Table 1. The present study found the mean age of the patients with HGGs was statistically significantly older than the patients with LGGs (p=0.028). Histopathological data of tumors are shown in Table 2.

Table 1. Demographic data of patients with LGGs and HGGs

Variables	LGGs+ (n=10)	HGGs++ (n=14)	p-value
Sex; n (%)			0.653
Male	2 (20.00)	5 (35.71)	
Female	8 (80.00)	9 (64.29)	
Age (years); mean±SD	42.1±14.65	60.38±21.12	0.028*

LGGs=low-grade gliomas; HGGs=high-grade gliomas; SD=standard deviation

+ CNS WHO grade 2; ++ CNS WHO grade 3 and 4

Table 2. Histopathological data of patients with LGGs and HGGs

Histopathology	n (%)
Low-grade gliomas (LGGs)	10 (41.67)
Astrocytoma, IDH mutant (WHO grade 2)	3 (12.50)
Astrocytoma, NOS (WHO grade 2)	5 (20.83)
Oligodendroglioma, IDH mutant and 1p/19q-codeleted (WHO grade 2)	2 (8.33)
High-grade gliomas (HGGs)	14 (58.33)
Glioblastoma, IDH wide-type	7 (29.17)
Glioblastoma, NOS	5 (20.83)
Astrocytoma, IDH mutant (WHO grade 3)	1 (4.17)
Oligodendroglioma, IDH mutant and 1p/19q-codeleted (WHO grade 3)	1 (4.17)

IDH mutant=isocitrate dehydrogenase gene mutation; NOS=not otherwise specified; 1p/19q-codeleted=loss of the short arm chromosome 1 and the long arm of chromosome 19

Table 3 reveals the MR characteristics of patients with LGGs and HGGs. Restricted diffusion was statistically more common in HGGs than LGGs (p=0.017), whereas other MR characteristics were not significantly different in both groups.

The statistically significant presence of hyperperfusion area on parametric maps of rCBV and rCBF from DSC-MRP in HGGs compared to LGGs was noted (p=0.010) with 92.86% sensitivity, 55.56% specificity, 76.47% PPV, 83.33% NPV, and 78.26% accuracy. HGGs also demonstrated significantly higher permeability on parametric maps of K^{trans}, V_e, and V_p than LGG (p=0.017) with 92.86% sensitivity, 50.00% specificity, 72.22% PPV, 83.33% NPV, and 75.00% accuracy. However, the presence of hyperperfusion area on the ASL-derived rCBF

Table 3. MRI Characteristics of patients with LGGs and HGGs

MRI characteristics	LGGs (n=10) n (%)	HGGs (n=14) n (%)	p-value
Margin			0.118
Well-defined	0 (0.00)	3 (21.43)	
Infiltrative	10 (100)	11 (78.57)	
T2/FLAIR mismatch			0.484
Absence	5 (50.00)	9 (64.29)	
Presence	5 (50.00)	5 (35.71)	
Cystic/necrotic area			0.633
Absence	3 (30.00)	3 (21.43)	
Presence	7 (70.00)	11 (78.57)	
Intratumoral signal void			0.188
Absence	7 (70.00)	6 (42.86)	
Presence	3 (30.00)	8 (57.14)	
Internal hemorrhage/calcification			0.301
Absence	3 (30.00)	1 (7.14)	
Petechial hemorrhage	4 (40.00)	6 (42.86)	
Gross hemorrhage (>1cm)	3 (30.00)	7 (50.00)	
Restricted diffusion			0.017*
Absence	5 (50.00)	1 (7.14)	
Presence	5 (50.00)	13 (92.86)	
Enhancement pattern			0.191
Absence	3 (30.00)	1 (7.14)	
Homogeneous	0 (0.00)	0 (0.00)	
Heterogeneous	7 (70.00)	11 (78.57)	
Ring enhancement	0 (0.00)	2 (14.29)	

LGGs=low-grade gliomas; HGGs=high-grade gliomas

map was not significantly different between the two groups (Table 4).

Interobserver agreement of the MR characteristics was almost perfect (Kappa value of 0.833 to 1.000) except for the enhancement pattern, which showed substantial agreement with a Kappa value of 0.712. For evaluation of each perfusion parametric map, Cohen's Kappa analysis demonstrated substantial agreement of all perfusion parameters (Kappa value of 0.649 to 0.800).

The ROC analysis to identify diagnostic value and optimal thresholds of DCE-, DSC-, and ASL-derived MRP parameters regarding the diagnosis of HGG and LGG is described in Table 5 and Figure 1. The DCE-derived V_p had the best diagnostic performance in differentiating between HGGs and LGGs (p=0.018) with AUC of 0.833, 100% sensitivity, 28.57% specificity, 70.59% PPV, and 100% NPV for the optimal cut-off value of 0.0002 mL/100 g. Statistically significant differences were also noted with the DCE-derived K^{trans} (p=0.011) and the DSC-derived normalized rCBV (p=0.021). Specifically, using the K^{trans} optimal cut-off value of 0.024 min^{-1} yielded an AUC of 0.750 (95% CI 0.527 to 0.973), 58.33% sensitivity, 100% specificity, 100% PPV, and 58.33% NPV, and using the DSC-derived normalized rCBV optimal cut-off value of 1.15 yielded an AUC of 0.750, 100% sensitivity, 37.50% specificity, 70.59% PPV, and 100% NPV. However, the ASL-derived normalized rCBF

Table 4. Diagnostic value of visual inspection of parametric maps of DCE-, DSC-, and ASL-derived perfusion parameters in patients with LGGs and HGGs

Parameters	Presence of hyperperfusion area or increased permeability			Diagnostic test				
	LGGs; n (%)	HGGs; n (%)	p-value	Sensitivity (95% CI)	Specificity (95% CI)	PPV (95% CI)	NPV (95% CI)	Accuracy (95% CI)
DCE (n=24)	(n=10)	(n=14)						
K^{trans}	5 (50.0)	13 (92.9)	0.017*	92.86% (66.1 to 99.8)	50.00% (18.7 to 81.3)	72.22% (46.5 to 90.3)	83.33% (35.9 to 99.6)	75.00% (53.3 to 90.2)
V_e	5 (50.0)	13 (92.9)	0.017*	92.86% (66.1 to 99.8)	50.00% (18.7 to 81.3)	72.22% (46.5 to 90.3)	83.33% (35.9 to 99.6)	75.00% (53.3 to 90.2)
V_p	5 (50.0)	13 (92.9)	0.017*	92.86% (66.1 to 99.8)	50.00% (18.7 to 81.3)	72.22% (46.5 to 90.3)	83.33% (35.9 to 99.6)	75.00% (53.3 to 90.2)
DSC (n=23)	(n=9)	(n=14)						
rCBV	4 (44.4)	13 (92.9)	0.010*	92.86% (66.1 to 99.8)	55.56% (21.2 to 86.3)	76.47% (50.1 to 93.2)	83.33% (35.9 to 99.6)	78.26% (56.3 to 92.5)
rCBF	4 (44.4)	13 (92.9)	0.010*	92.86% (66.1 to 99.8)	55.56% (21.2 to 86.3)	76.47% (50.1 to 93.2)	83.33% (35.9 to 99.6)	78.26% (56.3 to 92.5)
ASL (n=18)	(n=9)	(n=9)						
rCBF	4 (44.4)	6 (66.7)	0.343	66.67% (29.9 to 92.5)	55.56% (21.2 to 86.3)	60.00% (26.2 to 87.8)	62.50% (24.5 to 91.5)	61.11% (35.7 to 82.7)

LGGs=low-grade gliomas; HGGs high-grade gliomas; DCE=dynamic contrast-enhanced; DSC=dynamic susceptibility contrast; ASL=arterial spin labeling; K^{trans}=volume transfer coefficient; V_e=volume fraction of extravascular extracellular space; V_p=fractional blood plasma volume; rCBF=relative cerebral blood flow; rCBV=relative cerebral blood volume; PPV=positive predictive value; NPV=negative predictive value; CI=confidence interval

Table 5. Diagnostic value of quantitative DCE-, DSC-, and ASL-derived perfusion parameters for differentiation of LGGs and HGGs

Parameters	AUC (95% CI)	p-value	Diagnostic test						
			Cut-off value	Sensitivity (95% CI)	Specificity (95% CI)	PPV (95% CI)	NPV (95% CI)	Accuracy (95% CI)	p-value
DCE (n=19)									
K^{trans} (min^{-1})	0.750 (0.527 to 0.973)	0.076	0.024	58.33% (27.7 to 84.8)	100% (59.0 to 100.0)	100% (59.0 to 100.0)	58.33% (27.7 to 84.8)	73.68% (48.8 to 90.9)	0.011*
V_e	0.571 (0.277 to 0.866)	0.612	0.031	83.33% (51.6 to 97.9)	71.43% (29.0 to 96.3)	83.33% (51.6 to 97.9)	71.43% (29.0 to 96.3)	78.95% (54.4 to 93.9)	0.017*
V_p	0.833 (0.649 to 1.000)	0.018*	0.0002	100% (73.5 to 100.0)	28.57% (3.7 to 71.0)	70.59% (44.0 to 89.7)	100% (15.8 to 100.0)	73.68% (48.8 to 90.9)	0.050*
DSC (n=20)									
Normalized rCBV	0.750 (0.527 to 0.973)	0.064	1.15	100% (73.5 to 100.0)	37.50% (8.5 to 75.5)	70.59% (44.0 to 89.7)	100% (29.2 to 100.0)	75.00% (50.9 to 91.3)	0.021*
Normalized rCBF	0.688 (0.445 to 0.930)	0.165	1.02	100% (73.5 to 100.0)	37.50% (8.5 to 75.5)	70.59% (44.0 to 89.7)	100% (29.2 to 100.0)	75.00% (50.9 to 91.3)	0.021*
ASL (n=18)									
Normalized rCBF	0.457 (0.175 to 0.738)	0.757	1.12	77.78% (40.0 to 97.2)	44.44% (13.7 to 78.8)	58.33% (27.7 to 84.8)	66.67% (22.3 to 95.7)	61.11% (35.7 to 82.7)	0.317

LGGs=low-grade gliomas; HGGs high-grade gliomas; DCE=dynamic contrast-enhanced; DSC=dynamic susceptibility contrast; ASL=arterial spin labeling; K^{trans}=volume transfer coefficient; V_e=volume fraction of extravascular extracellular space; V_p=fractional blood plasma volume; rCBF=relative cerebral blood flow; rCBV=relative cerebral blood volume; AUC=area under the curve; PPV=positive predictive value; NPV=negative predictive value

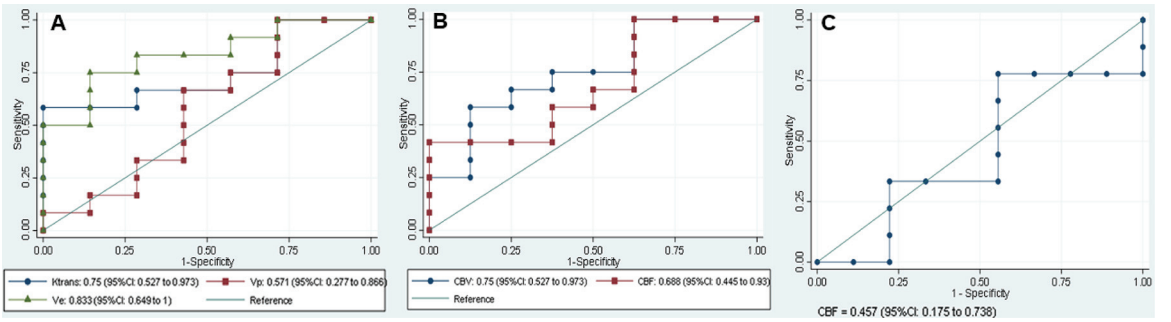

Figure 1. ROC curves of (A) DCE-derived Ktrans, Ve, Vp, (B) DSC-derived normalized rCBV, normalized rCBF and (C) ASL-derived normalized rCBF for differentiation of HGGs and LGGs.

demonstrated no statistically significant difference between HGGs and LGGs with an AUC of 0.457 (p=0.757).

Discussion

Providing a precise preoperative tumor grade assists the clinician in choosing proper management, including surgical and subsequent treatment protocols. Conventional MRI characteristics are not always accurate in differentiating HGGs from LGGs, as these two groups have overlapping imaging features[4].

In the present study, the presence of restricted diffusion within the tumor was the only conventional imaging feature that showed a statistically significant difference between HGGs and LGGs, which agrees with the previous studies by Kono et al.[25] and Fawzy et al.[26]. Meanwhile, other tumor characteristics on conventional MRI demonstrated no significant difference in determining the tumor grade, agreeing with the previous results by Nguyen et al.[13] and Pope et al.[27].

The utility of MRP for the differentiation of HGGs and LGGs is well recognized. The DCE-MRP, especially K^{trans}, provides information about microcirculation and neoangiogenesis of tumors, which can reflect the permeability of neovascular proliferation. Higher K^{trans} and V_p are indicative of HGGs. The DSC-MRP provides perfusion information of tumors based on the first pass of gadolinium through the capillary-bed inducing susceptibility effect. An increase in tumor vascularity and tumor grade correlate well with rCBV and rCBF. The ASL-MRP is a non-contrast technique providing perfusion information (rCBF) using arterial blood

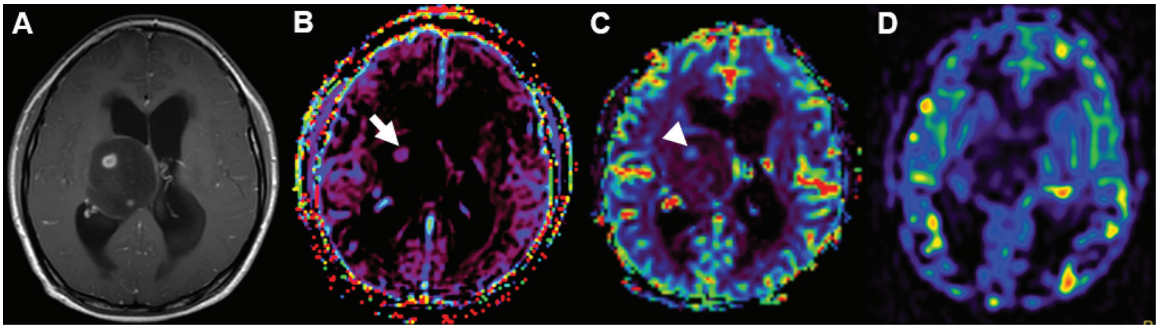

Figure 2. A 21-year-old woman with glioblastoma, NOS at the right thalamus showed two small enhancing foci within the mass on CE-T1W (A), increased permeability on DCE-Ktrans map (B, arrow) and focal area of hyperperfusion on DSC-rCBV map (C, arrowhead) but the absence of hyperperfusion on ASL-rCBF map (D).

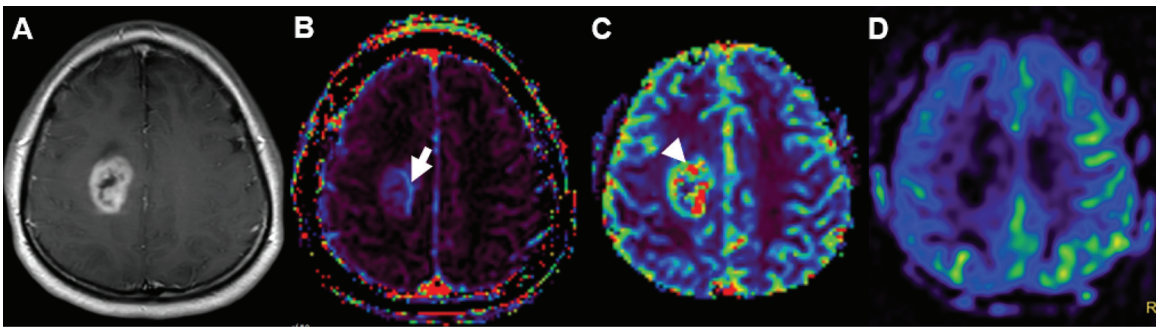

Figure 3. A 17-year-old woman with glioblastoma, NOS. (A) CE-T1W showed an irregular peripheral enhancing mass at the right frontoparietal region. (B, C) DCE-Ktrans map and DSC-rCBV map demonstrated increased permeability (B, arrow) and hyperperfusion (C, arrowhead). (D) ASL-rCBF revealed no hyperperfusion within the mass.

water as a freely diffusible endogenous tracer to help differentiate HGGs and LGGs. In the present study, DCE-derived V_p with the optimal cut-off value of 0.0002 mL/100g and K^{trans} with the optimal cut-off value of 0.024 min^{-1} have good diagnostic performance in differentiating between HGGs and LGGs. These two parameters might be imaging biomarkers for tumor neoangiogenesis and predict HGGs.

Qualitative assessment of increased perfusion or increased permeability within the tumor on the perfusion parametric map is widely used in routine clinical practice. In the present study, the ASL-derived rCBF visually inspected on a parametric map revealed no statistically significant difference between the two groups (p=0.343). The present study found three false-negative cases of pathologically proved HGGs that showed the absence of hyperperfusion area on the parametric map of rCBF in ASL-MRP but with the presence of hyperperfusion area on the parametric maps of DCE- and DSC-MRP (Figure 2, 3). Quantitative assessment of normalized rCBF also showed no statistical significance for differentiation of HGGs and LGGs in the present study with an AUC of 0.457 (95% CI 0.18 to 0.74) for the normalized rCBF of greater than 1.12, which achieved 77.78% sensitivity, 44.44% specificity, and 61.11% accuracy (p=0.317). ASL-MRP in the present study had a lower diagnostic value than the previous study by El Beheiry et al.[20], which yielded an AUC of 0.925 (95% CI 0.84 to 1.01) for rCBV greater than 2.08, 81.0% sensitivity, 85.7% specificity, 82.9% accuracy (p<0.001). On the contrary, previous studies on ASL-MRP, including a couple of meta-analyses by Falk Delgado et al.[17], showed the diagnostic performance of 0.9, summary sensitivity, and specificity of 89% and 80%, respectively. Previous ASL-MRP studied by Alsaedi et al.[16] revealed an AUC of 0.91 (95% CI 0.89 to 0.94), 86% sensitivity, and 84% specificity, which found that suboptimal inversion time (TI) might result in the lower diagnostic value of ASL.

The discrepancy between the present study and the previous studies could be due to difference in cut-off values, scanners, and ASL technical parameters. In the present study, the ASL-MRP has

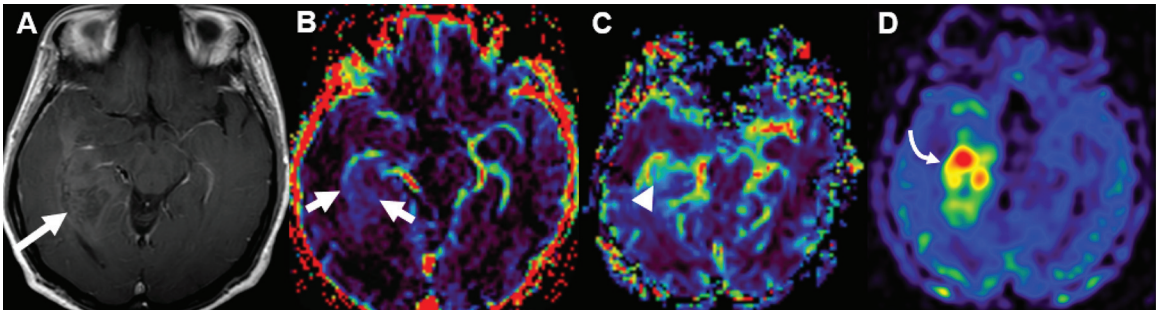

Figure 4. A 49-year-old woman with oligodendroglioma WHO grade 2 at the right temporal lobe. There was an ill-defined, faintly-enhancing mass on CE-T1W (A, long arrow), increased permeability on the DCE-Ktrans map (B, short arrows), hyperperfusion on DSC-rCBV map (C, arrowhead) and ASL-rCBF map (D, curve arrow) within the tumor.

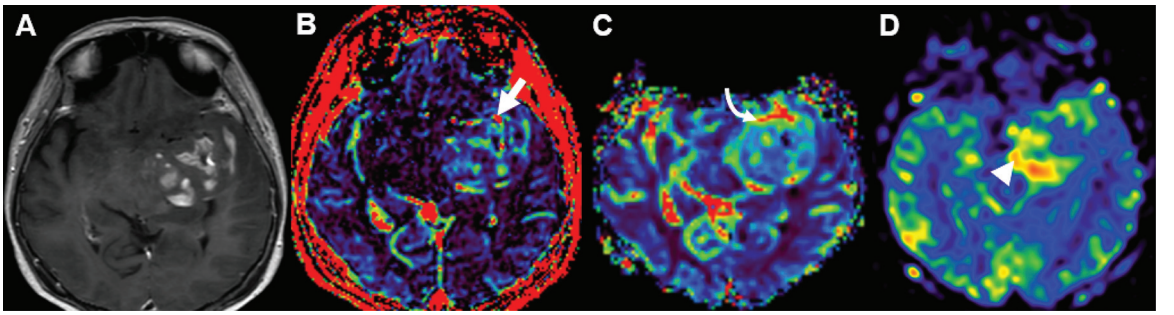

Figure 5. A 72-year-old woman with IDH mutant astrocytoma WHO grade 2, at the left temporal lobe seen as a multifocal irregular heterogeneous enhancing mass on CE-T1W (A), increased permeability on DCE-Ktrans map (B, arrow), hyperperfusion on DSC-rCBV map (C, curve arrow) and ASL-rCBF map (D, arrowhead) within the tumor.

a poor signal-to-noise ratio (SNR) and thicker slice compared with DCE- and DSC-MRP techniques, which could degrade the detection of the small area of hyperperfusion and result in a false negative on ASL-MRP.

The presence of increased perfusion or permeability on all parametric maps derived from DCE and DSC was significantly found in HGGs with high sensitivity of 92.86% in the present study. The results confirmed the usefulness of both DCE- and DSC-MRP in the preoperative assessment of gliomas and agreed with the studies published. However, the specificity and accuracy of all DCE- and DSC-derived parameters were lower than in the previous studies. The present study found five false-positive cases that showed increased perfusion or permeability on all parametric maps. These consisted of three cases of WHO grade 2 astrocytomas and two cases of WHO grade 2 oligodendrogliomas (Figure 4, 5). There were possible confounding effects from two cases of oligodendroglioma, which demonstrated increased perfusion or permeability on DCE- and DSC-MRP that could be explained by 1) the nature of oligodendroglioma, which often involves the cortical area, making it difficult to distinguish the adjacent cortical vessels from tumor neoangiogenesis, and 2) the microcapillary network known as chicken-wire pattern typically seen in low-grade oligodendrogliomas[14,28]. The elevated perfusion or permeability in oligodendrogliomas shown in the present study is in keeping with the previous result by Lev et al.[28].

After excluding the three cases, which were two benign and one malignant, of pathologically proven oligodendroglioma, the diagnostic performance of all MRP-derived parameters visually inspected on parametric maps was slightly improved, achieving 92.31% sensitivity (95% CI 64.0 to 99.8), 62.50% specificity (95% CI 24.5 to 91.5), and 80.95% accuracy (95% CI 58.1 to 94.6) for both DCE- and DSC-derived parameters. The diagnostic value of the ASL-derived parameter after the exclusion of oligodendroglioma cases was still inferior, with 75.00% sensitivity (95% CI 34.9 to 96.8), 71.43% specificity (95% CI 29.0 to 96.3), and 73.33% accuracy (95% CI 44.9 to 92.2).

There was one false-negative case in the present study, which was a case of astrocytoma

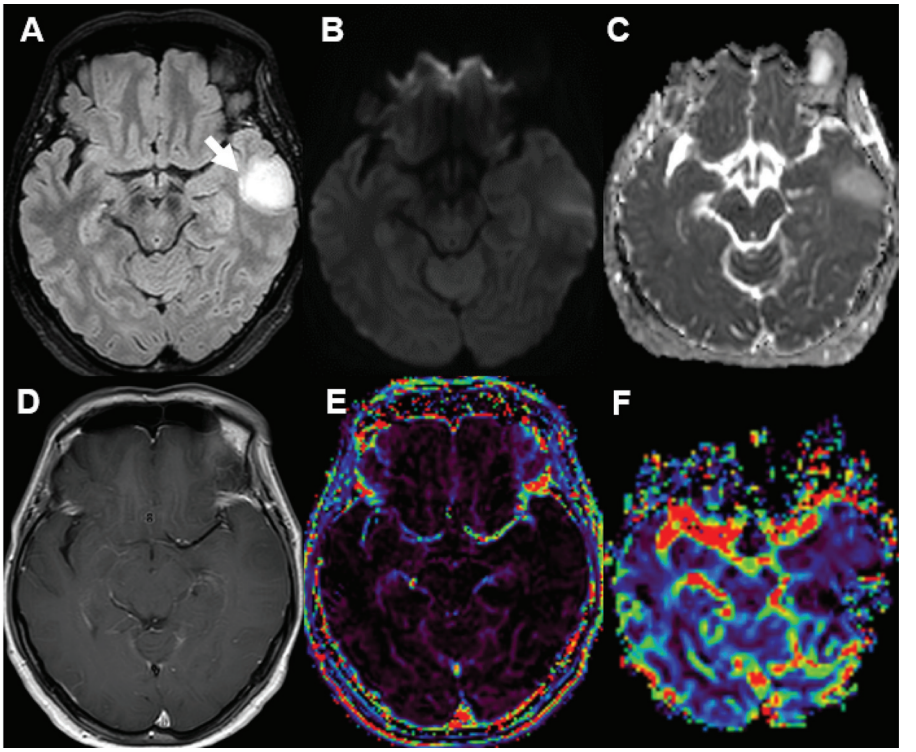

Figure 6. A 47-year-old woman with IDH mutant astrocytoma WHO grade 3. (A) CE-3D FLAIR/FS showed a homogeneous hyperintense mass at the left temporal lobe. (B, C) DWI and ADC images showed the absence of restricted diffusion. (D) CE-T1W showed no enhancement within the mass. (E, F) DCE-Ktrans and DSC-rCBV maps revealed the absence of increased permeability (E) and the absence of an area of hyperperfusion (F).

WHO grade 3, in which only the DSC- and DCE-perfusion techniques, and not the ASL technique, were performed (Figure 6). The discrepancies between conventional MR characteristics, MRP data and histopathology in this one false-negative case and the three false-positive cases could be attributed to the heterogeneity of these tumors.

Among the quantitative measurement of DCE- and DSC-derived parameters, the DCE-derived V_p demonstrated the highest AUC of 0.833 (95% CI 0.65 to 1), followed by DCE-derived K^{trans} and DSC-derived rCBV, with the latter two achieving similar AUC of 0.750 (95% CI 0.53 to 0.97). The present study demonstrated lower AUC, accuracy, and specificity than the previous studies[5-7,13,15]. In addition, no statistically significant difference between DCE-derived V_e and DSC-derived rCBF was found between HGGs and LGGs. Such findings were in disagreement with the previous meta-analysis conducted by Liang et al.[15], which showed statistical significance and high diagnostic performance in all DCE- and DSC-derived parameters, including K^{trans} (AUC 0.90, 95% CI 0.87 to 0.92, 88% sensitivity, and 80% specificity), V_e (AUC 0.88, 95% CI 0.85 to 0.91, 85% sensitivity, and 84% specificity), rCBV (AUC 0.93, 95% CI 0.90 to 0.95, 91% sensitivity, and 82% specificity), and rCBF (AUC 0.73, 95% CI 0.69 to 0.77, 88% sensitivity, and 68% specificity). The disagreement is affected by a small number of patients with only 24 patients, which consisted of five false-positive cases or 20.8% and one false-negative case or 4.2%, which is the main limitation of the present study.

Conclusion

DCE-derived V_p, DCE-derived K^{trans}, and DSC-derived rCBV are helpful perfusion MRI parameters for differentiation of HGGs and LGGs, with DCE-derived V_p showing the best diagnostic performance in this study.

What is already known on this topic?

- DCE MRP for differentiation of HGGs and LGGs.
- DSC MRP for differentiation of HGGs and LGGs.

What this study adds?

- Diagnostic value of MRP parameters obtained from DCE, DSC, and ASL to differentiate HGGs and LGGs.
- DCE-derived V_p, K^{trans}, and DSC-derived rCBV are helpful perfusion parameters in differentiating between HGGs and LGGs.
- DCE-derived V_p shows the best diagnostic performance in differentiating between HGGs and LGGs.

Acknowledgement

The authors would like to thank Mr. Dollapas Punpanich for her assistance with the statistical analysis.

Conflicts of interest

The authors declare no conflict of interest.

References

1. Ostrom QT, Patil N, Cioffi G, Waite K, Kruchko C, Barnholtz-Sloan JS. CBTRUS Statistical report: Primary brain and other central nervous system tumors diagnosed in the United States in 2013-2017. Neuro Oncol 2020;22:iv1-96.
2. Louis DN, Perry A, Wesseling P, Brat DJ, Cree IA, Figarella-Branger D, et al. The 2021 WHO Classification of Tumors of the Central Nervous System: a summary. Neuro Oncol 2021;23:1231-51.
3. Wang KY, Chen MM, Malayil Lincoln CM. Adult primary brain neoplasm, including 2016 World Health Organization Classification. Radiol Clin North Am 2019;57:1147-62.
4. Gharzeddine K, Hatzoglou V, Holodny AI, Young RJ. MR perfusion and MR spectroscopy of brain neoplasms. Radiol Clin North Am 2019;57:1177-88.
5. Okuchi S, Rojas-Garcia A, Ulyte A, Lopez I, Ušinskienė J, Lewis M, et al. Diagnostic accuracy of dynamic contrast-enhanced perfusion MRI in stratifying gliomas: A systematic review and meta-analysis. Cancer Med 2019;8:5564-73.
6. Jung SC, Yeom JA, Kim JH, Ryoo I, Kim SC, Shin H, et al. Glioma: Application of histogram analysis of pharmacokinetic parameters from T1-weighted dynamic contrast-enhanced MR imaging to tumor grading. AJNR Am J Neuroradiol 2014;35:1103-10.
7. Hilario A, Hernandez-Lain A, Sepulveda JM, Lagares A, Perez-Nuñez A, Ramos A. Perfusion MRI grading diffuse gliomas: Impact of permeability parameters on molecular biomarkers and survival. Neurocirugia (Astur: Engl Ed) 2019;30:11-8.
8. Zhang N, Zhang L, Qiu B, Meng L, Wang X, Hou BL. Correlation of volume transfer coefficient Ktrans with histopathologic grades of gliomas. J Magn Reson Imaging 2012;36:355-63.
9. Yan LF, Sun YZ, Zhao SS, Hu YC, Han Y, Li G, et al. Perfusion, diffusion, or brain tumor barrier integrity: Which represents the glioma features best? Cancer Manag Res 2019;11:9989-10000.
10. van Santwijk L, Kouwenberg V, Meijer F, Smits M, Henssen D. A systematic review and meta-analysis on the differentiation of glioma grade and mutational status by use of perfusion-based magnetic resonance imaging. Insights Imaging 2022;13:102.
11. Tran D, Nguyen DH, Nguyen HK, Nguyen-Thanh VA, Dong-Van H, Nguyen MD. Diagnostic performance of MRI perfusion and spectroscopy for brainstem glioma grading. Eur Rev Med Pharmacol Sci 2022;26:7938-48.
12. Arevalo-Perez J, Peck KK, Young RJ, Holodny AI, Karimi S, Lyo JK. Dynamic contrast-enhanced perfusion MRI and diffusion-weighted imaging in grading of gliomas. J Neuroimaging 2015;25:792-8.
13. Nguyen TB, Cron GO, Perdrizet K, Bezzina K, Torres CH, Chakraborty S, et al. Comparison of the diagnostic accuracy of DSC- and dynamic contrast-enhanced MRI in the preoperative grading of astrocytomas. AJNR Am J Neuroradiol 2015;36:2017-22.
14. Santarosa C, Castellano A, Conte GM, Cadioli M, Iadanza A, Terreni MR, et al. Dynamic contrast-enhanced and dynamic susceptibility contrast perfusion MR imaging for glioma grading: Preliminary comparison of vessel compartment and permeability parameters using hotspot and histogram analysis. Eur J Radiol 2016;85:1147-56.
15. Liang J, Liu D, Gao P, Zhang D, Chen H, Shi C, et al. Diagnostic values of DCE-MRI and DSC-MRI for differentiation between high-grade and low-grade gliomas: A comprehensive meta-analysis. Acad Radiol 2018;25:338-48.
16. Alsaedi A, Doniselli F, Jäger HR, Panovska-Griffiths J, Rojas-Garcia A, Golay X, et al. The value of arterial spin labelling in adults glioma grading: systematic review and meta-analysis. Oncotarget 2019;10:1589-601.
17. Falk Delgado A, De Luca F, van Westen D, Falk Delgado A. Arterial spin labeling MR imaging for differentiation between high- and low-grade glioma-a meta-analysis. Neuro Oncol 2018;20:1450-61.
18. Ferré JC, Bannier E, Raoult H, Mineur G, Carsin-Nicol B, Gauvrit JY. Arterial spin labeling (ASL) perfusion: techniques and clinical use. Diagn Interv Imaging 2013;94:1211-23.
19. Fu J, Li L, Wang X, Zhang M, Zhang Y, Li Z. Clinical utility of arterial spin labeling for preoperative grading of glioma. Biosci Rep 2018;38:BSR20180507.
20. ElBeheiry AA, Emara DM, Abdel-Latif AAB, Abbas M, Ismail AS. Arterial spin labeling in the grading of brain gliomas: could it help? Egypt J Radiol Nucl Med 2020;51:235.
21. Louis DN, Perry A, Reifenberger G, von Deimling A, Figarella-Branger D, Cavenee WK, et al. The 2016 World Health Organization Classification of Tumors

of the Central Nervous System: A summary. Acta Neuropathol 2016;131:803-20.
22. Tofts PS, Brix G, Buckley DL, Evelhoch JL, Henderson E, Knopp MV, et al. Estimating kinetic parameters from dynamic contrast-enhanced T(1)-weighted MRI of a diffusable tracer: standardized quantities and symbols. J Magn Reson Imaging 1999;10:223-32.
23. Petrella JR, Provenzale JM. MR perfusion imaging of the brain: techniques and applications. AJR Am J Roentgenol 2000;175:207-19.
24. Deguchi S, Oishi T, Mitsuya K, Kakuda Y, Endo M, Sugino T, et al. Clinicopathological analysis of T2-FLAIR mismatch sign in lower-grade gliomas. Sci Rep 2020;10:10113.
25. Kono K, Inoue Y, Nakayama K, Shakudo M, Morino M, Ohata K, et al. The role of diffusion-weighted imaging in patients with brain tumors. AJNR Am J Neuroradiol 2001;22:1081-8.
26. Fawzy FM, Almassry HN, Ismail AM. Preoperative glioma grading by MR diffusion and MR spectroscopic imaging. Egypt J Radiol Nucl Med 2016;47:1539-48.
27. Pope WB, Brandal G. Conventional and advanced magnetic resonance imaging in patients with high-grade glioma. Q J Nucl Med Mol Imaging 2018;62:239-53.
28. Lev MH, Ozsunar Y, Henson JW, Rasheed AA, Barest GD, Harsh GRt, et al. Glial tumor grading and outcome prediction using dynamic spin-echo MR susceptibility mapping compared with conventional contrast-enhanced MR: confounding effect of elevated rCBV of oligodendrogliomas [corrected]. AJNR Am J Neuroradiol 2004;25:214-21.